

Neurochemical Comparison of Synaptic Arrangements of Parvocellular, Magnocellular, and Koniocellular Geniculate Pathways in Owl Monkey (*Aotus trivirgatus*) Visual Cortex

YURI SHOSTAK,¹ YUCHUAN DING,^{1,2} AND VIVIEN A. CASAGRANDE^{1,3*}

¹Department of Cell and Developmental Biology, Vanderbilt University, Nashville, Tennessee 37232

²Department of Neurological Surgery, Wayne State University Medical School, Detroit, Michigan 48201

³Departments of Psychology, and Ophthalmology and Visual Sciences, Vanderbilt University, Nashville, Tennessee 37232

ABSTRACT

As in other primates, the lateral geniculate nucleus (LGN) of owl monkeys contains three anatomically and physiologically distinct relay cell classes, the magnocellular (M), parvocellular (P), and koniocellular (K) cells. M and P LGN cells send axons to the upper and lower tiers of layer IV, and K cells send axons to the cytochrome oxidase (CO) blobs of layer III and to layer I of primary visual cortex (V1). Our objective was to compare the synaptic arrangements made by these axon classes. M, P, and K axons were labeled in adult owl monkeys by means of injections of wheat germ agglutinin-horseradish peroxidase into the appropriate LGN layers. The neurochemical content of both pre- and postsynaptic profiles were identified by postembedding immunocytochemistry for γ -aminobutyric acid (GABA) and glutamate. Our key finding is that the synaptic arrangements made by M, P, and K axons in owl monkey exhibit more similarities than differences. They are exclusively presynaptic, contain glutamate and form asymmetric synapses mainly with glutamate-positive dendritic spines. The majority of the remaining axons synapse with glutamatergic dendritic shafts. There are also differences between LGN pathways. M and P terminals are significantly larger and more likely to make multiple synapses than K axons, although M and P axons do not differ from each other in either of these characteristics. Of interest, a larger percentage of M and K axons than P axons make synapses with GABAergic dendritic shafts. Cells directly postsynaptic to M and K axons are known to exhibit orientation selectivity and, in some cases, direction selectivity. Cells postsynaptic to P axons do not show these properties, but instead tend to reflect their LGN inputs more faithfully; therefore, it is possible that these physiologic differences seen in the cortical cells postsynaptic to different LGN pathways reflect the differential involvement of inhibitory circuits. *J. Comp. Neurol.* 456:12–28, 2003.

© 2002 Wiley-Liss, Inc.

Indexing terms: GABA; glutamate; immunocytochemistry; primate; striate cortex; electron microscopy

Grant sponsor: National Institute of Health; Grant numbers: EY01778 (V.A.C.); EY08126; HD15052.

*Correspondence to: Vivien A. Casagrande, Department of Cell and Developmental Biology, Vanderbilt University Medical School, Medical Center North B2323, Nashville, TN 37232-2175.
E-mail: vivien.casagrande@vanderbilt.edu

Received 4 December 2001; Revised 9 July 2002; Accepted 1 August 2002
DOI 10.1002/cne.10436

Published online the week of December 9, 2002 in Wiley InterScience (www.interscience.wiley.com).

Visual signals to primary visual cortex (V1) in primates arrive by means of three parallel pathways from the lateral geniculate nucleus (LGN), the magnocellular (M), parvocellular (P), and koniocellular (K) pathways (see Casagrande, 1994, for review). Evidence in several primate species, including owl monkeys (subjects of this study), suggests that these pathways transmit distinct spatial and temporal information from the retina to V1 (Sherman et al., 1976; Casagrande and Norton, 1991; Merigan and Maunsell, 1993; Xu et al., 2001). The synaptic arrangements present within the layers and compartments of primary visual cortex (V1) combine and amplify signals arriving from the parallel LGN pathways. This process results in the construction of cells with a variety of new receptive field properties that are distinct from their LGN inputs. Examples of such properties include sharp orientation and direction tuning, binocularity, disparity tuning, and a variety of more complex properties (for review, see Sompolinsky and Shapley, 1997). Many of these properties are distinct from those found at the level of the LGN regardless of the pathway; LGN cells are typically monocular with simple ON-center/OFF-surround or the reverse receptive field organization but can differ in spatial and temporal resolution (Casagrande and Norton, 1991). What remains puzzling is that, in simian primates, some target cells of LGN afferents respond identically to their LGN inputs, whereas others exhibit more complex receptive field properties, such as sharp orientation tuning. This finding means that the complex properties exhibited by cortical neurons must be constructed in at least two different ways. These properties could be constructed either directly at the LGN target cell or at the next level. If the properties are combined at the target, then they result from: 1) the unique arrangement of LGN afferents as originally proposed by Hubel and Wiesel (1962) (see also Ferster, 1988), 2) they are based upon intrinsic wiring, or 3) some combination. In simian primates, data indicate that cortical layer IV β cells postsynaptic to P LGN axons have receptive fields that are similar or identical to their LGN inputs, whereas targets of M LGN axons in layer IV α and cell targets of K LGN axons in the layer III CO blobs do not (see Merigan and Maunsell, 1993, for review). From these observations and the fact that the laminar composition and circuitry of V1 cortical layers differ, one would predict that the microcircuitry involving P, M, and K LGN axons would also differ.

At present, surprisingly little is known about the synaptic arrangements and neurochemistry of different LGN axon classes or the microcircuitry of LGN target neurons in primates. Studies of the synaptic circuitry of primate LGN input pathways have mainly examined M and P inputs to layer IV in macaque monkeys (Garey and Powell, 1971; Tigges and Tigges, 1979; Winfield and Powell, 1983; Freund et al., 1989). Only two studies have examined the synaptic circuitry of the K pathways in layer III CO-blobs (Ding and Casagrande, 1998; Shostak et al., 2002). These studies generally agree that M, P, and K axons mainly synapse with dendritic spines with a significant minority synapsing with dendritic shafts and very few synapsing with somata (Tigges and Tigges, 1979; Freund et al., 1989; Ding and Casagrande, 1998; Shostak et al., 2002). No studies, however, have directly compared the synaptic arrangements made by all three classes of LGN axon in the same species. Also, few details are available concerning the neurochemical content of elements

postsynaptic to primate LGN axons with the exception of K LGN axons (Garey and Powell, 1971; Tigges and Tigges, 1979; Winfield and Powell, 1983; Freund et al., 1989; Ding and Casagrande, 1998; Shostak et al., 2002).

In light of the above evidence, our overall objective was to compare the synaptic arrangements and neurochemistry of the different LGN axon classes and the microcircuitry of LGN target neurons. We used the owl monkey for this study, both because its visual system is well studied (Casagrande and Kaas, 1994; O'Keefe et al., 1998; Xu et al., 2001) and because we have detailed knowledge from our own work on the termination and neurochemical synaptic arrangement of K axons in V1 (Ding and Casagrande, 1997, 1998; Shostak et al., 2002).

MATERIALS AND METHODS

Two owl monkeys (*Aotus trivirgatus*) were used to examine synaptic circuits of the magnocellular (M) and parvocellular (P) LGN axons within the cortical layers IV α and IV β , respectively. Because M and P LGN cell axons have been found to project exclusively to IV α and IV β , respectively (Kaas et al., 1976; Diamond et al., 1985; Pospichal et al., 1994; Ding and Casagrande, 1997, 1998), iontophoretic injections of wheat germ agglutinin conjugated to horseradish peroxidase (WGA-HRP) were made into M and P LGN layers in the same animal. Detailed data on synaptic circuits of K LGN axons in V1 were obtained from the same cases used in a previous study (Ding and Casagrande, 1998). All of the monkeys were cared for according to the National Institutes of Health Guide for the Care and Use of Laboratory Animals and the guidelines of the Vanderbilt University Animal Care and Use Committee. The nomenclature used to identify owl monkey LGN and cortical layers has been described previously (see Ding and Casagrande, 1997).

Surgical procedures

All surgical procedures were carried out under aseptic conditions while the animals were deeply anesthetized. Before surgery, atropine sulfate (0.1 mg/kg) was given to inhibit salivation. The owl monkeys then were intubated, anesthetized with isoflurane (3–4%) in oxygen, and maintained with the same gas mixture at 1–2%. Heart and respiration rates were continuously monitored, and reflexes were tested periodically; animals were kept warm with a water-circulating heating pad throughout surgery. Once deeply anesthetized, the monkeys were secured in a stereotaxic apparatus, the skull exposed and a craniotomy performed.

Labeling LGN cell axons

A dural flap was elevated and 5% agar in saline was spread over the pial surface to prevent desiccation. For identification of the LGN layers, evoked responses to a flashing light were recorded from the LGN through an electrode glued to a pipette (20–30 μ m inner tip diameter) filled with 1% WGA-HRP in saline. LGN layers were identified on the basis of changes in eye dominance and relative position in the LGN. The tracer was iontophoretically injected for 30 minutes (3 seconds ON/3 seconds OFF, 3–5 μ A). Because M and P LGN cell axons project exclusively to cortical layer IV α or IV β (Diamond et al., 1985; Ding and Casagrande, 1997) and K axons project to CO-blobs and layer I, it was not necessary to limit the injections to

a single LGN layer. Instead, large LGN injections of WGA-HRP were made within LGN layer K3, which involved the adjacent M and P layers. After the injections, the dural flap was repositioned and the skin was sutured.

Postoperatively, animals were given 0.02 mg/kg of Bannamine as an analgesic and 300,000 units/kg of a long-acting penicillin (Flocillin) and monitored carefully until they were fully conscious and capable of eating and drinking on their own. At this point, they were returned to their home cages and provided with soft palatable foods and water. Details of the surgery were similar to those described earlier (Lachica and Casagrande, 1992; Ding and Casagrande, 1997, 1998).

Histologic procedures and WGA-HRP histochemistry

After a 2-day survival period, the animals were deeply anesthetized with an overdose of Nembutal (50 mg/kg) and perfused transcardially with a brief rinse of oxygenated saline followed by 2% paraformaldehyde/1.5% glutaraldehyde in 0.1 M phosphate buffer (pH 7.4) at 4°C. Animals were then perfused with the fixative containing 4% sucrose. The brains were removed and post-fixed in 4% sucrose/fixative at 4°C for 1 hour. They were then rinsed in three changes of 0.1 M phosphate buffer (pH 7.4) and placed in 4% sucrose in the same buffer at 4°C overnight. The following day, the visual cortex was blocked anterior to V2 and was dissected from the remainder of the cortical hemisphere. Then, parasagittal 60- μ m sections were cut on a Vibratome. The thalamus was removed and sectioned parasagittally at 52 μ m on a freezing microtome.

All cortical and LGN sections were treated according to a modified tetramethyl benzidine (TMB) stabilization procedure (Mesulam, 1978; Horn and Hoffman, 1987). Sections were then mounted on gelatin-coated slides, air-dried, dipped briefly in a clearing agent (Histo-Clear), and cover-slipped. Counterstaining was unnecessary in these cases, because LGN and cortical layers were clearly visible in the TMB-reacted sections.

Electron microscopic preparation and postembedding immunocytochemistry

Tissue preparation for electron microscopy. Processed sections with labeled axons were treated with 1% osmium tetroxide in 0.1 M phosphate buffer at 4°C and dehydrated in graded ethanols into propylene oxide and then infiltrated with Epon resins overnight. After polymerizing at 60°C for 2 days, tissue containing WGA-HRP labeled M or P axons from cortical layer IV α or IV β was removed with a NeuroPunch (Ted Pella). These neuropunches were centered on the layer IV α or IV β . A small portion of other layers might have been included within these original punches, but these other layers were later removed when the block was trimmed before ultrathin sectioning.

Postembedding immunocytochemistry for glutamate and GABA. Ultrathin sections (60–70 nm) were cut with a diamond knife and mounted on single-slot nickel grids. Modified techniques originally described by Phend et al. (1992) to optimize postembedding double staining for glutamate and GABA immunocytochemistry were used in this study. Briefly, ultrathin sections were rinsed for 5 minutes in TBST (0.05 M Tris, 0.1% Triton X-100, pH 7.6). Sections on grids were incubated in 1:300 polyclonal primary anti-glutamate (raised in rabbits, Chemicon, Inc.)

overnight. After rinsing in TBST, pH 7.6, and in TBST, pH 8.2, sections were incubated in a secondary antibody, goat anti-rabbit immunoglobulin (Ig) G conjugated to gold (10 nm, BioCell) diluted 1:20 in TBST, pH 8.2 for 1–2 hours. After completion of the glutamate immunostaining, binding sites were deactivated over paraformaldehyde vapors in an 80°C oven for 1 hour. Sections were then incubated 24–48 hours at a 1:500 dilution of a polyclonal anti-GABA antibody (raised in rabbits, Sigma), followed by incubation in a goat anti-rabbit IgG-conjugated to gold (20 nm, BioCell) secondary antibody, diluted 1:40, for 1–2 hours. The sections then were rinsed first in TBST (pH 7.6), then in deionized water, and were finally stained with uranyl acetate and lead citrate.

Controls. The specificities of glutamate or GABA antibodies were evaluated by preabsorbing the primary antibodies with an excess of glutamate-BSA conjugate or GABA-conjugate, respectively. Immunostaining for the appropriate antibody was eliminated in these controls. Additional controls involved the application of rabbit pre-immune serum, as well as processing a series of immunoreactions in which various steps were omitted from the regular staining sequence. In these controls, the immunoreactivity was almost completely abolished.

Data collection and analysis

All LGN injection sites were reconstructed from serial sections by using a microprojector at low magnification (170 \times) to document the location and extent of the WGA-HRP label. Injection site boundaries were defined as those zones containing a dark focus of the label.

Grids were viewed on a Hitachi H 800 electron microscope at 100 kV. Sections were examined and photographed at 15,000 \times , the original negatives were scanned with an Epson Es 1200c scanner, and digital images were compiled in Adobe Photoshop version 6.0. Data were collected by selecting WGA-HRP-labeled terminals with postsynaptic elements. We measured only WGA-HRP-labeled LGN terminals that had clear pre- and postsynaptic profiles. Labeled terminals that did not make synapses were not measured. No effort was made to serially section every bouton to determine the exact number of synapses made by each. We used the term “multiple synapses” when single LGN axons are synapsing with several different postsynaptic profiles.

In the present study, we used the criteria proposed originally by Freund et al. (1989) to distinguish dendritic spines from small dendritic shafts. According to these criteria, all dendritic profiles that contain mitochondria and/or microtubules are classified as dendritic shafts, regardless of their diameter, and all small profiles lacking mitochondria and microtubules are classified as dendritic spines. Because glutamatergic terminals characteristically make asymmetric synapses and GABAergic terminals make symmetric synapses, we divided profiles into these morphologic categories before estimating the signal and noise levels of our gold-labeled material. Ten-nanometer gold particles were used to identify the presence of glutamate, and 20-nm gold particles were used to identify the presence of GABA. Ten to 14 randomly selected morphologically defined profiles (see above) were measured at a magnification of 15,000 \times . The number of profile-associated small and large gold particles was counted and related to the area of the profiles. The areas of the morphologically identified profiles were measured

TABLE 1. Number of Gold Particles per μm^2

Cell type	No. of large gold particles	No. of small gold particles	Profile area (μm^2)	No. of profiles
Glutamatergic	0.64 ± 0.23	28.43 ± 4.58	0.96 ± 0.21	N = 14
GABAergic ¹	14.1 ± 2.85	14.8 ± 3.11	0.99 ± 0.19	N = 10

¹GABA, γ -aminobutyric acid.

by using an isotropic uniform random test system (lattice) of quadrants (Cruz-Orive and Wiebel, 1981; Cruze-Orive, 1989). We found (see Table 1) that the background labeling (large gold particles) for profiles making asymmetric synaptic junctions (glutamatergic) was 0.64 ± 0.23 particles per $1 \mu\text{m}^2$. In profiles making symmetric synaptic junctions defined as positive labeling for GABA, we found 14.1 ± 2.85 large gold particles per $1 \mu\text{m}^2$ ($P < 0.0001$, t test). We found that background labeling (small gold particles) for profiles making symmetric synaptic junctions (GABAergic) was 14.8 ± 3.11 particles per $1 \mu\text{m}^2$. In profiles making asymmetric synaptic junctions defined as positive labeling for glutamate, we found 28.43 ± 4.58 particles per $1 \mu\text{m}^2$ ($P = 0.034$, t test). Therefore, pre- and postsynaptic profiles were considered immunoreactive for glutamate if they contained at least 24 particles per $1 \mu\text{m}^2$. Profiles were considered immunoreactive for GABA if they contained at least 11 particles per $1 \mu\text{m}^2$.

As a measure of synaptic efficacy, we quantified the areas of each terminal bouton. Many other measures could be used such as size of the active zone or numbers of synaptic vesicles, but the latter measures have not been found to correlate any better with synaptic release than bouton size (Pierce and Mendell, 1993). In fact, in the spinal cord, Pierce and Mendell (1993) showed that several morphologic features associated with synaptic release (including the sizes of synaptic plaques, mitochondrial volume, vesicle number, active zone vesicle number, apposed surface, active zone area, bouton surface area, as well as the sizes of postsynaptic profiles) scale directly in proportion to bouton size. In addition, Hamos et al. (1987) revealed that, although boutons arising from a single retinogeniculate axon varied considerably in size, active zone number correlated well with bouton volume, reinforcing the idea that bouton size is a meaningful measure even in the visual system. For this analysis, the cross-sectional areas of all labeled terminals in which both pre- and postsynaptic profiles were distinct were measured by tracing the contour of the profiles by using the BioQuant-IV image analysis system (R&M Biometrics, Inc., Nashville, TN). The size of the local area, containing single labeled profiles, was $42.56 \mu\text{m}^2$ for all measurements, and sizes of labeled profiles were in the range of 0.6 – $3.9 \mu\text{m}^2$; therefore, relative sizes of counted profiles were 1.4 – 9.2% of the total measured area in each layer of visual cortex (total measured area for layer III = $5,575.36 \mu\text{m}^2$, for layer IV α = $7,490.56 \mu\text{m}^2$, and for layer IV β = $8,895.04 \mu\text{m}^2$).

RESULTS

Our key result was that the synaptic arrangements made by LGN M, P, and K axons in owl monkey visual cortex share many common features. Nevertheless, interesting qualitative and quantitative differences were found

in the relationship of these axons to GABAergic profiles, in the numbers of elements postsynaptic to M, P, and K LGN axons that receive other inputs, and in the sizes of the terminals. These similarities and differences are described in more detail below.

Injection sites and cortical projections of the M and P LGN axons

The general pattern of geniculocortical projections from the individual layers of the LGN in owl monkeys has been reported previously (Kaas et al., 1976; Diamond et al., 1985; Pospichal et al., 1994; Ding and Casagrande, 1997, 1998). Results show that, in owl monkeys as in other primates, M LGN axons terminate primarily within cortical layers IV α and VI, and K axons terminate within the CO blobs of layers III and in layer I of V1. P axons only terminate within layer IV β (and possibly layer VI) and do not have the separate termination site within layer IIIB β (IVA of Brodmann, 1909) seen in squirrel monkeys and macaque monkeys (see Casagrande and Kaas, 1994, for review). In the present study, a large injection of WGA-HRP that involved all LGN layers confirmed this original pattern (data not shown). A dense continuous band of the label was evident in layer IV at the site corresponding retinotopically to the center of the injection. At the edges of these termination sites in layer IV, it was common to find differences in the relative density of the label within IV α and IV β that presumably reflected differences in the relative spread of the label into P or M LGN layers at the edge of the injection site. Even though tissue from these edge regions was not examined at the ultrastructural level, these differences viewed at the light microscopic level provided a useful guide to determine the boundaries of terminations of M vs. P axons. Above layer IV, distinct patchy label was seen within layer III with a central focus in sublayer IIIB α . From our previous studies, we know that these patches of the label reflect the input from K LGN axons and that they coincide with the location of the CO blobs within this layer (Diamond et al., 1985; Ding and Casagrande, 1997, 1998; Shostak et al., 2002).

Contribution of LGN M axons to synaptic circuits in V1

One hundred seventy-six WGA-HRP-labeled M axon terminals identified by the presence of an electron-dense reaction product in cortical layer IV were examined (Figs. 1–5). These geniculocortical terminals contained five or more mitochondria, were packed with clear round vesicles, and all were immunopositive for glutamate. Immunopositive profiles containing glutamate were identified by the presence of small (10 nm) gold particles (smaller gold particles are indicated by thin arrows in Figs. 1–5); none of these terminals were immunoreactive for GABA (identified by large [20-nm] gold particles, as indicated by arrowheads in Figs. 1–5). LGN axon terminals formed extended asymmetric synaptic junctions with dendritic profiles, both spines and shafts, but not with cell bodies. By using the criteria of Freund et al. (1989), we determined that 72% of M axons synapsed with dendritic spines (Figs. 1, 5), and the remainder synapsed with small and large dendritic shafts (Figs. 2B, 3). We observed that small dendritic shafts postsynaptic to geniculate axons frequently contained a mitochondrion and a lamellar body adjacent to the synaptic contact. One example of such small shafts is shown in synaptic contact with a labeled M

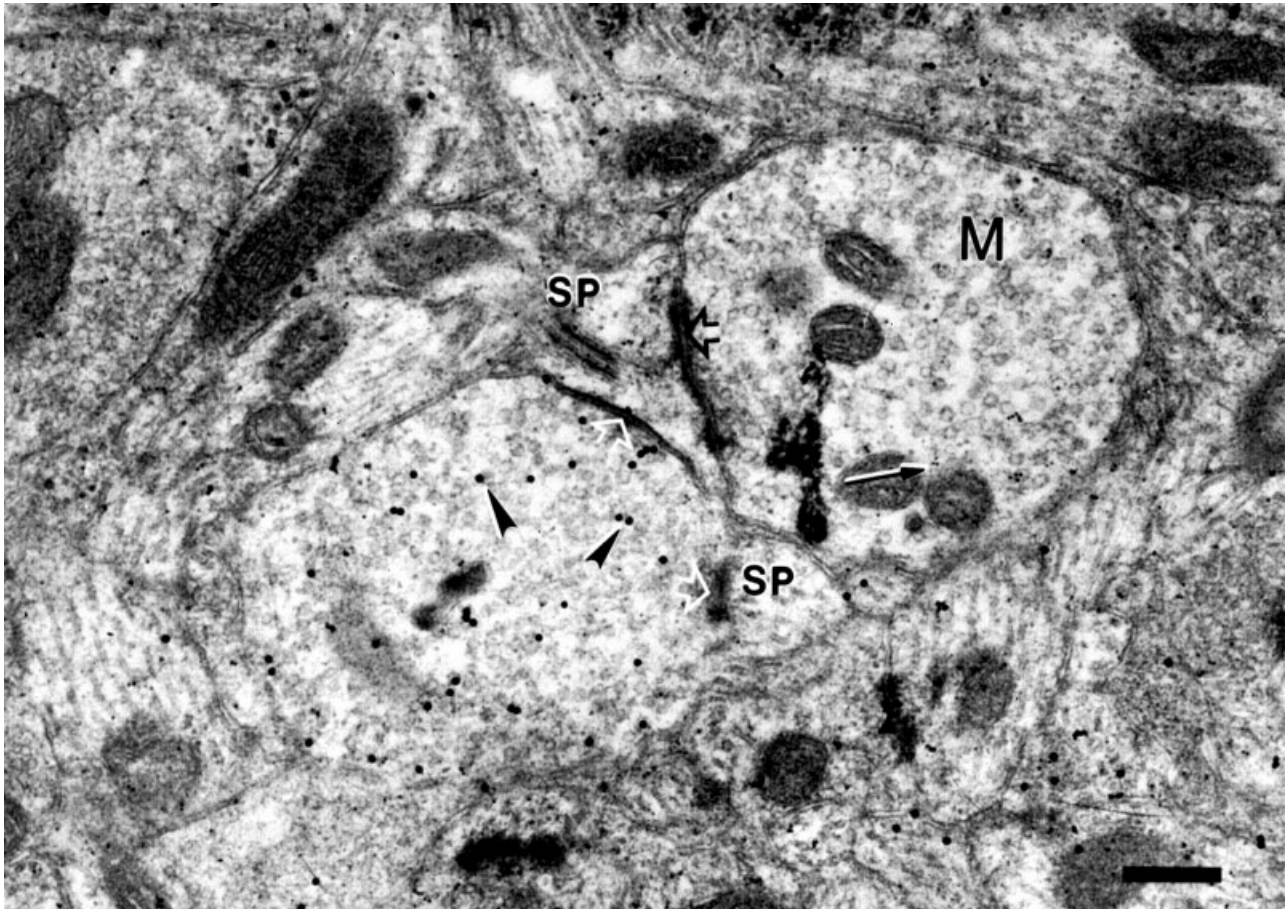


Fig. 1. Wheat germ agglutinin-horseradish peroxidase-labeled lateral geniculate nucleus magnocellular axon terminals in layer IV α (indicated by M) were identified by electron-dense reaction product. Many M axons make asymmetric synapses (an example is indicated by a black open arrow) with dendritic spines (indicated by sp). Note that one of two spines labeled with sp show clear examples of a spine apparatus. M axons use glutamate (small black dots; examples are indicated by thin black arrow) as a neurotransmitter and synapse

with glutamatergic dendritic spines. Larger gold particles (20 nm) showing immunoreactivity for γ -aminobutyric acid (GABA) are seen as larger black dots (examples are indicated by black arrowheads). M axons make synapses with spines that also receive a symmetric synapse (white open arrowheads) from a GABAergic profile. Note that the lower sp profile may have microtubules, although the plane of section makes it difficult to say for sure; therefore, that profile also could be considered a small dendrite. Scale bar = 0.5 μ m.

terminal in Figure 3A. Although lamellar bodies are virtually indistinguishable from spine apparatusi in macaque monkeys, Freund et al. (1989) have shown through serial reconstructions that such small dendritic profiles containing mitochondria are never spines. In our material, such lamellar bodies were only seen in the smallest glutamate-positive dendritic shafts (Fig. 3A). The vast majority (93%) of the postsynaptic dendritic spines were immunoreactive for glutamate (Fig. 5). The remainder of postsynaptic spines contained no label. Sixty-five percent of dendritic shafts contacted by M terminals were immunoreactive for glutamate (Fig. 3), and the rest were immunoreactive for GABA (Fig. 4).

Unlike K axons, which generally synapse with single postsynaptic profiles (Ding and Casagrande, 1998; Shostak et al., 2002), M axons engaged in both single and multiple synaptic contacts with either a dendritic spine or a dendritic shaft, or both. M axons made synapses with two or three dendritic spines (Fig. 2A), with one dendritic spine and one shaft (Figs. 2B, 5) or with two dendritic

shafts (Fig. 4). In our material, 21% of M axons made such multiple synapses. Obviously, this percentage of multiple synapses is likely to be an underestimate given that serial sectioning was not performed and that many M axons are at least 2.0 μ m in diameter.

Some of the dendritic spines that received synaptic input from M axons also received symmetric synaptic input from GABA-positive axonal profiles. Figure 1 shows a clear example of a spine containing a distinct spine apparatus receiving synapses from both an M axon and a GABAergic axon from an interneuron. The GABA-positive axon, in turn, makes a synaptic junction (seen cut obliquely) with another small dendritic spine that is in very close proximity to the M terminal. One characteristic of synaptic relationships involving M axons was the complex association with profiles from other sources, particularly GABAergic profiles. Thirty-two percent of the total elements postsynaptic to M terminals (both spines and shafts) received at least one additional synapse from other sources. Twenty-five percent of all elements postsynaptic

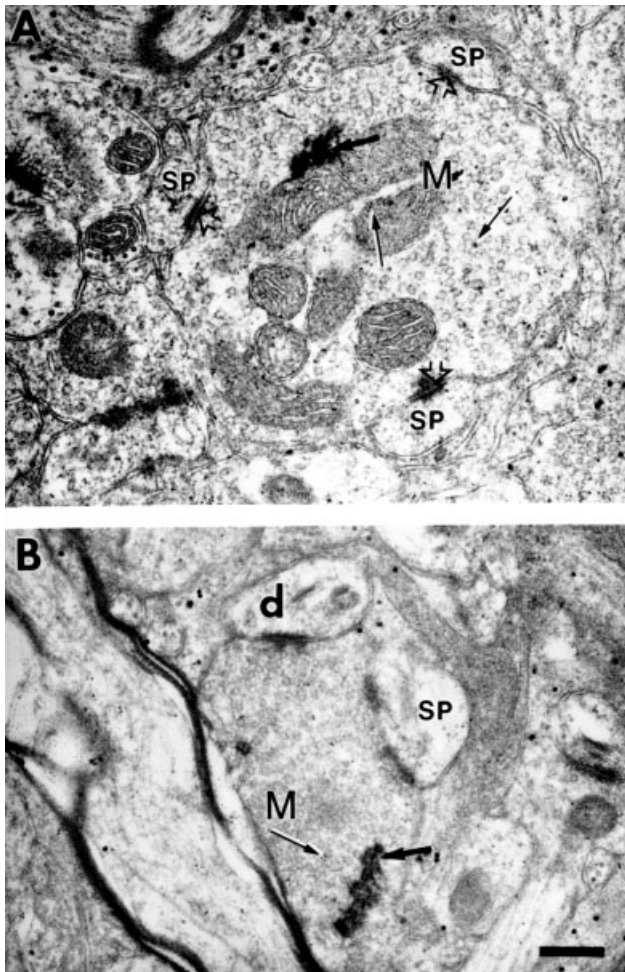


Fig. 2. **A:** Many large magnocellular (M) axons make asymmetric synapses (open arrowheads) with more than one spine (SP). Single M axons can make synapses with both dendritic spines and shafts. **B:** Profiles that contained mitochondria were classified as dendritic (d) shafts. Thick black arrow indicates WGA-HRP label. Other conventions are as in Figure 1. Scale bar = 0.5 μm in B (applies to A,B).

to M terminals (both spines and shafts) received at least one additional synapse from a GABAergic profile. Several larger postsynaptic dendritic shafts (positive for either glutamate or GABA, but typically GABA) received input from GABAergic axons (Fig. 4), although the dendrites could also receive asymmetric synapses from other glutamatergic axons (Fig. 4). Of interest, when dendritic spines postsynaptic to M axons received additional synaptic input, it was always from a GABAergic profile (Fig. 1).

Contribution of LGN P axons to synaptic circuits in V1

Two hundred and nine terminals were identified as WGA-HRP-labeled axons from LGN P layers based on the electron dense reaction product (Figs. 6–10). Like both M and K pathways, all labeled axons from LGN P layers in our material were immunopositive for glutamate, identified as described earlier (Figs. 6–10). P axon terminals, like M axons, were characterized by relatively tightly

packed, round vesicles, and the majority contained five or more profiles of mitochondria. Also, like M and K axons, all of the synapses observed between labeled P axons and postsynaptic elements were asymmetric and the majority (77%) of P axons synapsed with dendritic spines (Fig. 6), with the remainder synapsing with dendritic shafts (Figs. 7–10). The bulk (93%) of spines postsynaptic to P cell axons were immunoreactive for glutamate (Fig. 6) and the remainder were unlabeled. As in the case with M axons, small dendritic shafts that contain lamellar bodies were seen postsynaptic to P axons. A clear example is shown in Figure 8 where a labeled P terminal makes a synapse with a small dendritic shaft that contains both a mitochondrion and a lamellar body. The lamellar body in this case lies directly opposite an adherence junction that appears almost as an extension of the synapse. Qualitatively, lamellar bodies were seen less frequently in small dendritic shafts in synaptic association with either P or K axons than with M axons. The vast majority (86%) of dendritic shafts receiving contacts from labeled P axons contained glutamate (Figs. 7, 8), and the rest were immunoreactive for GABA (Fig. 9). None of the identified P axons were found to synapse with a cell body or another axon.

Labeled LGN axon terminals from P layers were exclusively presynaptic, forming single and multiple synapses with dendritic profiles, as seen in the M pathway. Although complete serial sections of these labeled boutons would be required to be certain, 19% of P boutons appeared to have multiple synapses with dendritic profiles. Labeled P axons were seen making synaptic junctions with two or more postsynaptic profiles, such as two or three spines (Fig. 6B), one spine and one shaft (Fig. 6C), or two shafts (Fig. 7). When dendritic spines postsynaptic to P axons had an additional input, it was exclusively from a GABAergic source (Figs. 6A, 8). Also, labeled P profiles and other unlabeled axonal profiles (presumably glutamatergic or GABAergic) were seen in synaptic contact with the same dendritic shaft (glutamatergic or GABAergic) (Fig. 9). However, it was less common to find that elements postsynaptic to P axons receiving other contacts, particularly from GABAergic profiles, than was the case for M axons. Twenty percent of all elements postsynaptic to P terminals (both spines and shafts) received one or more additional synapses from other sources, and only 13% of all elements postsynaptic to P terminals (both spines and shafts) received an additional synapse from a GABAergic profile (Fig. 11C).

Comparisons between M, P, and K synaptic arrangements

We found that M and P axons engaged in more complex synaptic arrangements than did K axons. In particular, M and P axons terminated more often than K axons in regions that contained complicated synaptic zones uninterrupted by glial lamellae resembling synaptic arrangements in the LGN (Guillery 1969, 1971). Examples of complex synaptic zones involving the M and P pathways are shown in Figure 10A,B, and for the K pathway in Figure 12 (see also Figs. 4, 6C).

In an effort to better document similarities and differences between the synaptic arrangements made by M, P, and K axon classes, we made several additional measurements. When we restricted our analysis simply to postsynaptic dendrites, we found that M axons had more interactions with GABAergic interneurons than K axons and that P axons had the fewest interactions. Thirty-five percent of

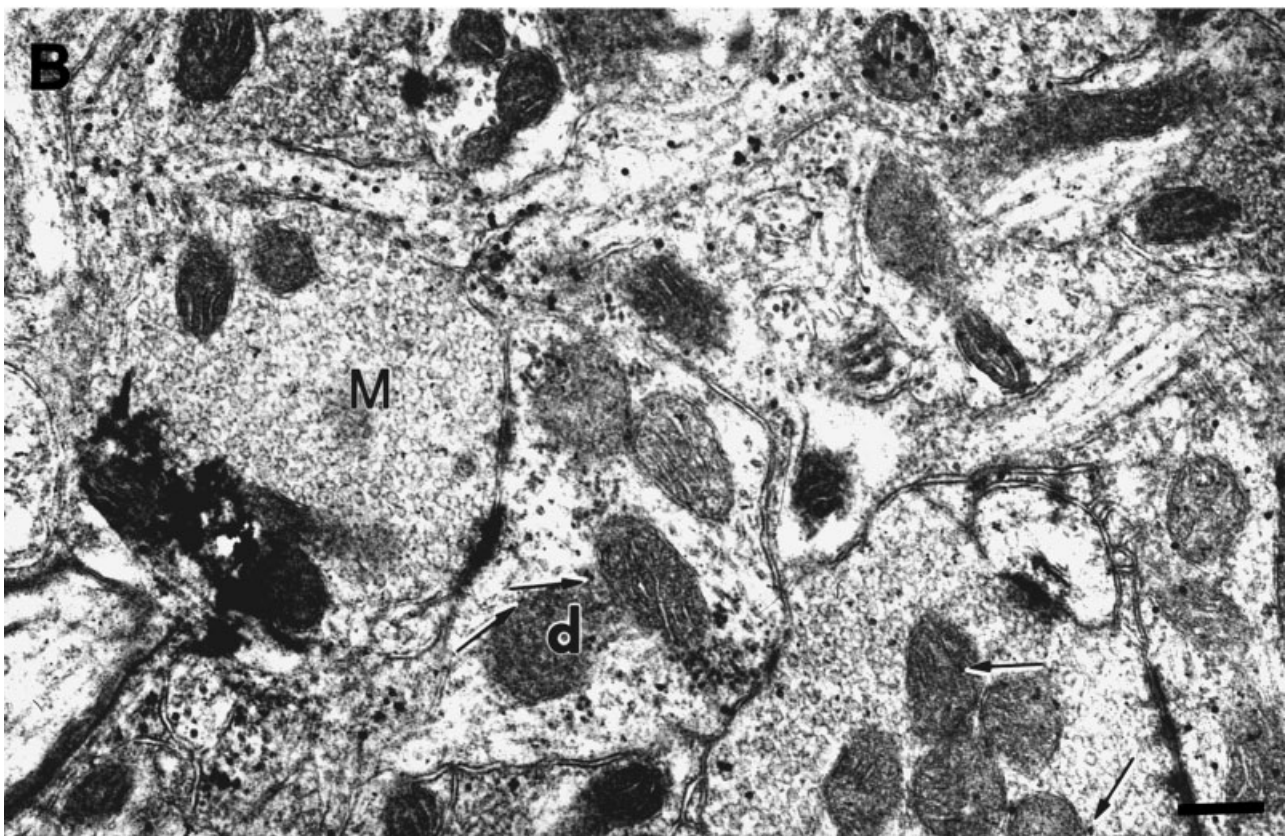
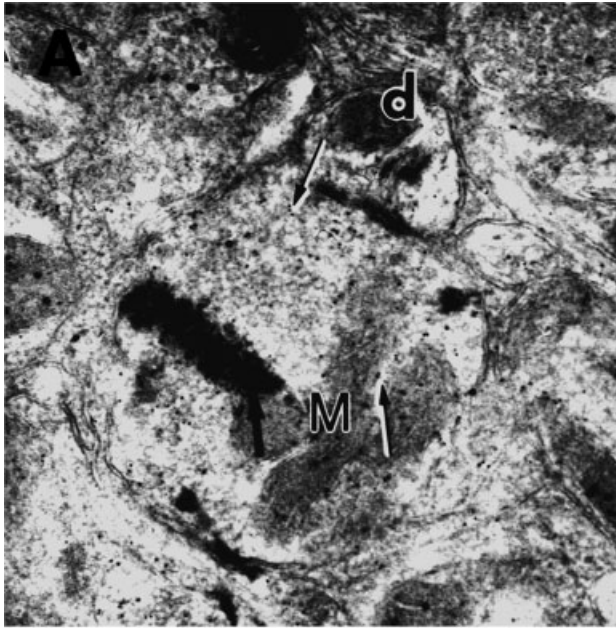


Fig. 3. A significant minority of M axons synapse with dendritic (d) shafts. **A:** Small dendritic shafts postsynaptic to geniculate axons frequently contain a mitochondrion and a lamellar body adjacent to the synaptic junction. In the example shown in A, the M axon and

dendrite not only form a synaptic junction but exhibit an adherence junction adjacent to the synaptic junction. **B:** M axons also were found to synapse with larger dendritic shafts. Other conventions are as in Figures 1 and 2. Scale bar = 0.5 μm in B (applies to A,B).

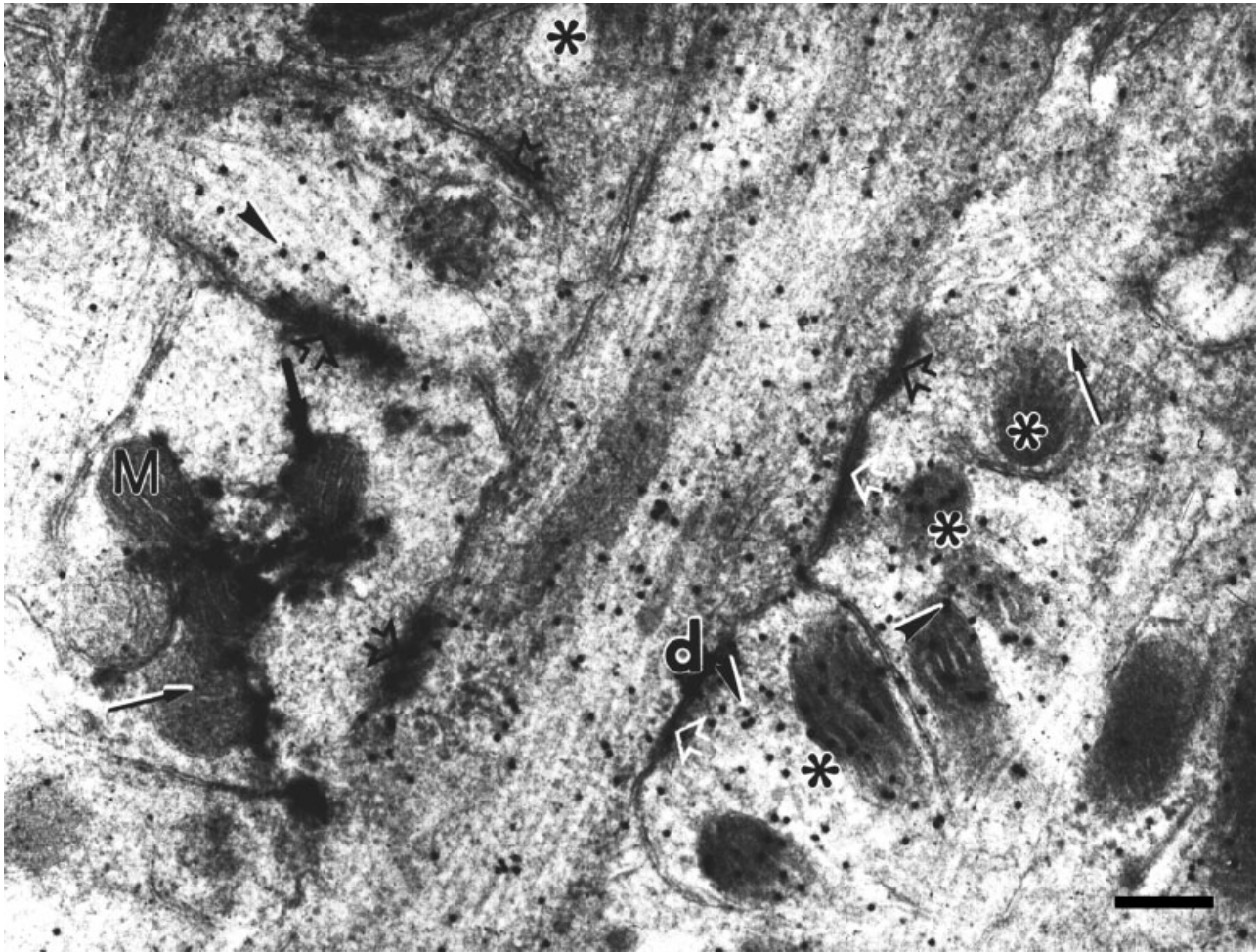


Fig. 4. M axons also have complex synaptic associations with GABAergic profiles. A labeled M axon makes a synaptic junction with two GABAergic (large gold particles indicated by solid black arrowheads) dendritic shafts. Both dendritic shafts receive synapses from other profiles, indicated by asterisks containing either GABA or glutamate. Other conventions are as in Figures 1 and 2. Scale bar = 0.5 μm .

M synapses were made with GABAergic dendrites, whereas K and P axons made 26% and 14% of their synapses with these profiles (Fig. 13).

In addition, we evaluated four other parameters: terminal size, the percentage of multiple synapses made by each terminal, the percentage of postsynaptic profiles receiving other synapses, and the type of postsynaptic profile contacted by each class of LGN axon. Figure 11A shows the percentage of LGN terminal profiles that fall into different size categories. M and P axons showed surprisingly similar distributions, with terminals ranging in size from 0.6 to 3.9 μm^2 in area. The peak for P axons, between 0.9 and 1.2 μm^2 (27%), was somewhat smaller than the peak for M axons at 1.2–1.5 μm^2 (22%). K axon terminals ranged in size from 0.1 to 1.2 μm^2 with the peak at 0.3–0.6 μm^2 in size (55%). The average terminal areas of M axons ($\bar{x} = 1.40 \pm 0.65 \mu\text{m}^2$, $n = 176$) and P axons ($\bar{x} = 1.29 \pm 0.54 \mu\text{m}^2$, $n = 209$) were significantly larger (t test, $P \leq 0.00001$ for M and K; $P \leq 0.0001$ for P and K) than K axon terminal areas ($\bar{x} = 0.51 \pm 0.36 \mu\text{m}^2$, $n = 131$).

Figure 11B compares the percentages of M, P, and K axons that make multiple synapses with postsynaptic pro-

files. It is clear from this comparison that M axons (21%) and P axons (19%) made more multiple synapses than K axons (only 4%) did. Again, it is important to point out that these comparisons were performed on single sections; serial section reconstructions are likely to yield higher percentages. Figure 11C documents the percentages of postsynaptic profiles contacted by LGN M, P, and K axons receiving other inputs. More elements postsynaptic to M axons were found to receive additional inputs (32%), than those postsynaptic to P (20%) or K axons (13%). Finally, we quantified the types of postsynaptic elements contacted by M, P, and K axons. Seventy-two percent of M axons, 77% of P axons, and 61% of K axons terminated on dendritic spines, most of which could be identified as glutamatergic. The remainder terminated on dendritic shafts (Fig. 11D).

DISCUSSION

Our key finding is that the synaptic arrangements made by M, P, and K axons in owl monkey exhibit more



Fig. 5. In this example, a large M terminal makes a synapse with both a glutamate-positive spine (small gold particles indicated by thin black arrows) and a GABA-positive dendritic shaft (large gold particles indicated by filled black arrowheads). The GABAergic dendrite, in turn, receives an asymmetric synapse (open black arrowheads) from another profile indicated by an asterisk. Other conventions are as in Figures 1 and 2. Scale bar = 0.5 μ m.

fundamental similarities than differences. This finding is despite the fact that each axon class arises from a distinct LGN cell type and ends within V1 layers that contain cells with different functional properties and connections. Nevertheless, there are differences between pathways, especially in the degree to which each LGN axon class engages the inhibitory (GABAergic) elements of V1, that could bear significantly on the function of postsynaptic cells. In the discussion that follows, we compare our results with the findings of others and consider the implications of the similarities and differences we have documented in the synaptic arrangements of LGN M, P, and K pathways.

Similarities between M, P, and K synaptic arrangements

In owl monkeys, as in other primates, there are clear physiological differences between the response properties of the LGN M and P layer cells (Sherman et al., 1976). K LGN cells in owl monkeys also display unique receptive field properties (Xu et al., 2001). Because the separation of M, P, and K pathways is maintained all the way to the first synapse in the cortex, it is somewhat surprising that we did not uncover more major differences between these pathways at the first synapse. Our data show that in owl monkeys M, P, and K LGN axons contain glutamate and synapse exclusively with dendrites. The majority of each axon type synapses with dendritic spines, and 90% or more of these geniculocortical axons synapse with dendrites that contain glutamate. These characteristics of geniculocortical axons in owl monkeys also have been described in other species, suggesting that these are general features of mammalian LGN axons regardless of type (Garey and Powell, 1971; Winfield et al., 1982; Freund et al., 1989).

With the exception of K axons (Ding and Casagrande, 1998; Shostak et al., 2002), direct immunocytochemical confirmation of the presence of glutamate in geniculocortical axons has not been reported for other primates. The proposal that all of these axons use glutamate is reinforced by many studies demonstrating that geniculate relay cells or geniculocortical axons in other mammals contain glutamate (Hata et al., 1988; Montero, 1990, 1994; Kharazia and Weinberg, 1994). Spines appear to be the preferred targets of geniculocortical axons in owl monkeys, as well as other species. In owl monkeys, M, P, and K axons contact spines 72%, 77%, and 61% of the time, respectively (also see Ding and Casagrande, 1998). In macaque monkeys, comparable numbers have been reported for the M and P axons. By using the same criteria for spine identification, Freund et al. (1989) found that 52–69% of M and P axons in macaque monkeys synapse with spines in layer IV. Other investigators, by using more liberal criteria for defining a spine, have reported that up to 90% of M and P axons synapse with dendritic spines in layer IV in macaque and squirrel monkeys (Garey and Powell, 1971; Tigges and Tigges, 1979; Winfield et al., 1982; Winfield and Powell, 1983). Most spine-bearing cells contain an excitatory transmitter (Greenamyre and Porter, 1994; Nieuwenhuys, 1994). In layer IV of macaque monkeys, dendritic spines postsynaptic to M and P axons are exclusively immunonegative for GABA (Freund et al., 1989) or have been directly identified as belonging to presumed excitatory spiny stellate neurons (Garey and Powell, 1971; Winfield et al., 1982). Also, 80% of dendritic shafts postsynaptic to macaque M and P terminals in layer IV are presumed to be excitatory based on immunonegativity for GABA. Consequently, just as in owl monkeys, approximately 90% of elements postsynaptic to M and P axons have been identified as excitatory in macaque monkeys (Freund et al., 1989). In cats, X and Y geniculocortical axons terminating in visual areas 17 and 18 contact dendritic spines and shafts of excitatory cells almost exclusively, as do geniculocortical axons within area 17 of rats (Garey and Powell, 1971; LeVay and Gilbert, 1976; Winfield and Powell, 1976, 1983; Peters and Feldman, 1977; Freund et al., 1985a,b; Kharazia and Weinberg, 1994). Together, these findings suggest that geniculate

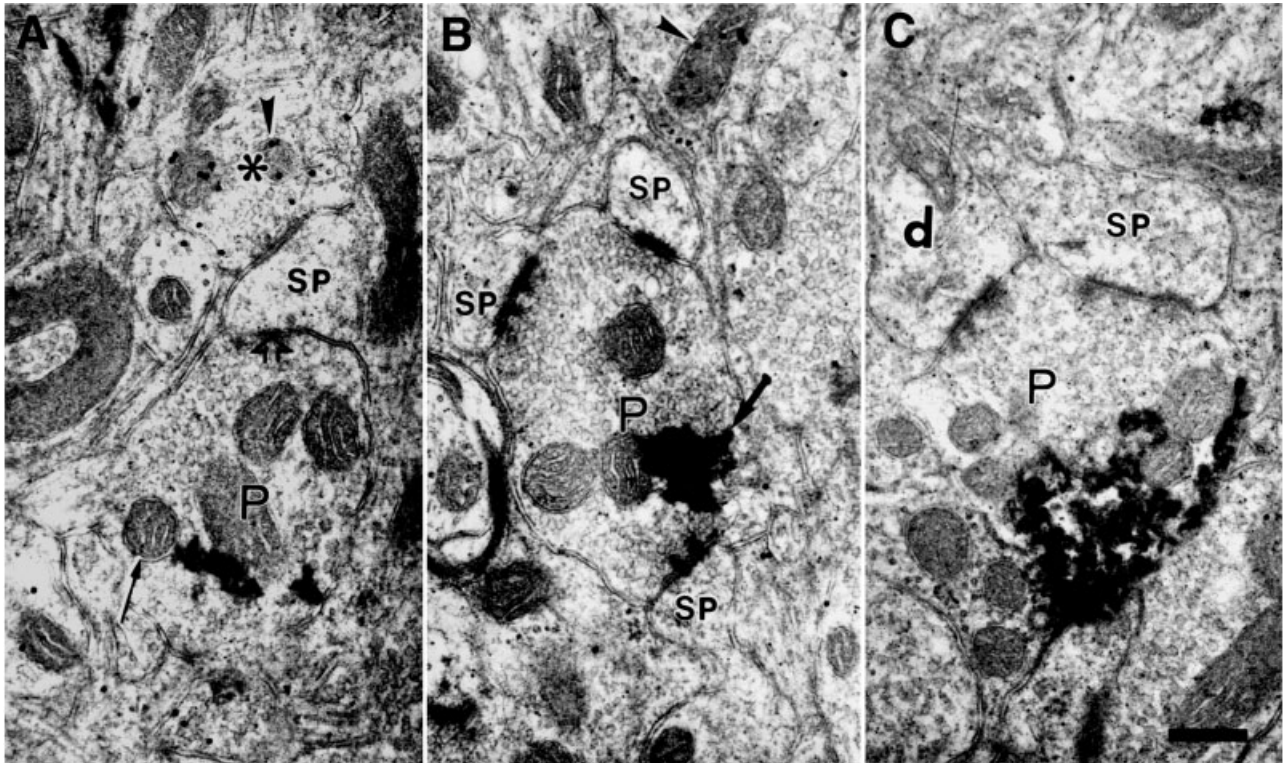


Fig. 6. Parvocellular (P) axons in layer IV β contain glutamate (small gold particles indicated by thin black arrows) and synapse mainly with dendritic spines (A). Single P axons can be found that synapse with one spine (A), two or more spines (B), or spines and

dendritic shafts (C). Spines that receive synapses from P axons receive another synapse from a GABAergic axon indicated by an asterisk in A. Other conventions are as in Figures 1 and 2. Scale bar = 0.5 μ m in C (applies to A–C).

relay cells and their cortical targets, regardless of class, use glutamate to communicate signals through the first synapse.

There are other similarities between the P and M synaptic arrangements in owl monkeys and in macaque monkeys. Our data show that M and P axon terminals in owl monkeys are approximately the same size, although the median for M terminals is slightly larger (Fig. 11A). There is, however, one caveat that should be added. It is possible that some of our labeled axons were actually collaterals of corticogeniculate cells within layer VI that also project to layer IV (see Katz, 1987; Wiser and Callaway, 1996). Although there is no direct support in any primates for the existence of such collaterals, there are data in cat to suggest that some corticogeniculate projection cells also have axon collaterals in layer IV. We do not believe contamination from recurrent collaterals represents a problem for our data for the following reasons. If these recurrent axons from corticogeniculate axons exist in primates, they are likely to occur in only a small percentage of cells, because intracellular filling in slices showed that only 2 of the 7 classes of cells identified within macaque monkey layer VI have both recurrent collaterals in layer IV and an axon that also exits toward the white matter (Wiser and Callaway, 1996). Because axons exiting in the white matter reflect both cells sending an axon to the LGN and cells sending axons to the claustrum, this number is still smaller. Second, although we did see a few retrogradely labeled cells in layer VI below our punches, the majority of

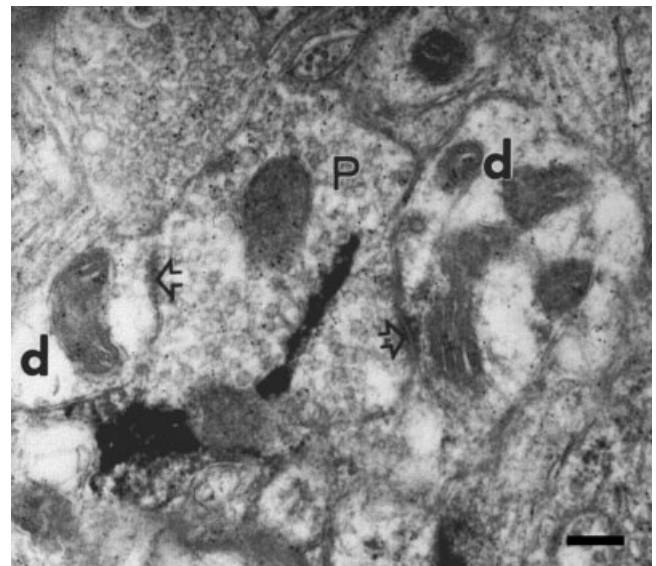


Fig. 7. A significant minority of parvocellular (P) axons synapse with dendritic shafts. P axons can synapse with two or more dendritic shafts of different sizes. Other conventions are as in Figure 1. Scale bar = 0.5 μ m.

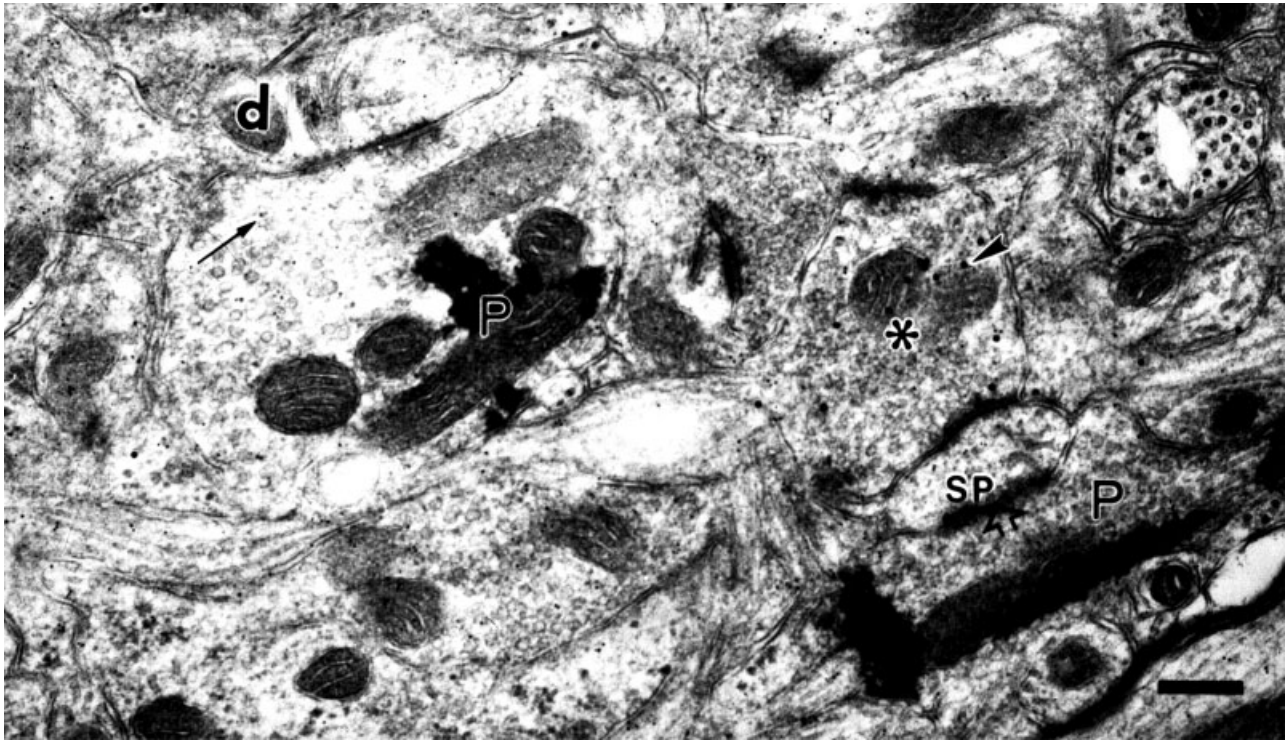


Fig. 8. Several small dendritic shafts postsynaptic to parvocellular (P) axons contain lamellar bodies that lie directly opposite to an adherence junction, which in this figure appears directly adjacent to a synaptic junction. The P axon shown here lies within a field contain-

ing complex synaptic relationships between several small glutamatergic profiles and one GABAergic profile (asterisk). Other conventions are as in Figure 1. Scale bar = 0.5 μm .

these cells were only lightly labeled without evidence of any processes. Even if a small fraction of our filled axons represented filled recurrent collateral boutons from layer VI, it is likely that these boutons are smaller in area than boutons in layer IV from the LGN. In cats, these recurrent axons were found to have boutons in the range of 0.3–1.0 μm in diameter and electron microscopic data, presented by Freund and colleagues (1985a), showed that Y axons in layer IV are in the range of 3–4 μm in diameter and X axons are in the range of 1.5–2.5 μm in diameter. If we assume that the same *proportional* size difference reported for cats exists between recurrent collaterals and geniculocortical terminals in layer IV in primates, we can estimate the proportion of our P and M bouton sizes in layer IV that may have been contaminated by the addition of potential collateral terminals from cells in layer VI. The effect of eliminating this proportion of our size range makes the differences between M and P vs. K axon terminals, presented in our Figure 11A, even more dramatic.

Approximately the same percentage of M and P terminals, 21% and 19%, respectively, make multiple synapses with postsynaptic targets. In studies of single sections (comparable to this study), 24% of M axons and 15% of P axons in macaque monkeys were found to make multiple synapses (Winfield et al., 1982). In serial sections, the same investigators report that these percentages rose to 82% and 27%, respectively. The number of synapses has been correlated to bouton size, with the larger M boutons making more synapses than the smaller P boutons. In owl monkeys, where our data indicate that M and P axons

have approximately the same mean size, the number of boutons made by each class is also similar, whereas the number of multiple synapses made by the smaller K axon terminals is significantly less. Thus, the larger size of LGN boutons in owl monkeys also appears to correlate with a greater tendency to make multiple synapses.

Differences between M, P, and K synaptic arrangements

Despite the number of similarities between the synaptic arrangements made by M, P, and K axons, there are also interesting differences. A key difference concerns the relationship of each of these axon classes to GABAergic profiles. According to our data, M axons exhibit the strongest association with such inhibitory profiles, and P axons exhibit the least, with K axons falling between. Twice as many K axons as P axons synapse directly with GABAergic dendrites and 1.5 times as many M as K axons synapse with GABAergic profiles, suggesting that M axons have a much higher tendency to be involved in inhibitory networks than K or P axons. This result is surprising, because such differences were not reported for M and P axons (K axons were not examined) in macaque monkeys (Freund et al., 1989). In macaque monkeys, Freund et al. (1989) examined two aspects of GABAergic circuitry. First, they compared the innervation of GABAergic neurons in layer IV by LGN M and P axons and found no differences. Second, they examined the relationship between the thalamic and GABAergic input to the same neuron. As we show in owl monkeys, GABAergic synapses

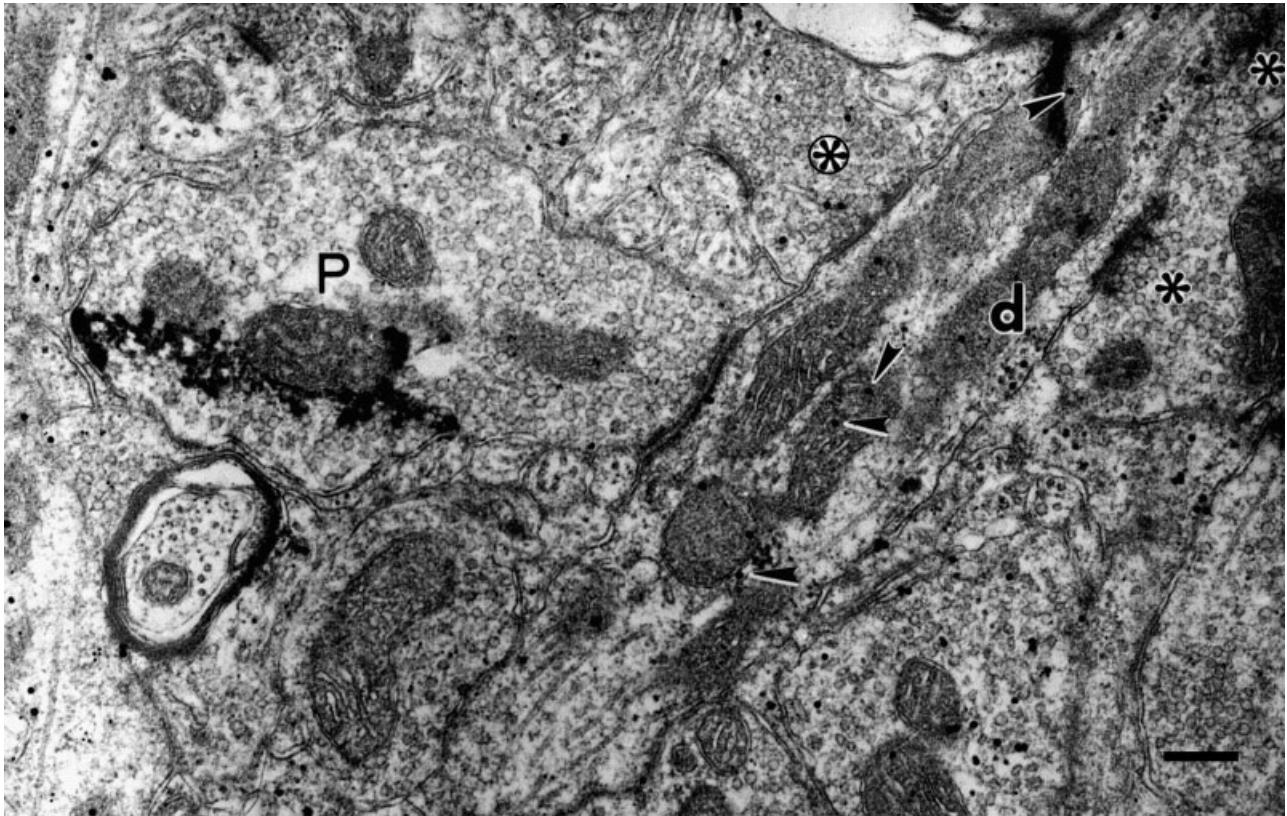


Fig. 9. Parvocellular (P) axons also synapse with GABAergic dendritic shafts. A labeled P axon synapses with a GABAergic dendrite (d) that also receives synaptic input from two glutamatergic profiles (asterisks) and one GABAergic profile (circled asterisk). Other conventions are as in Figure 1. Scale bar = 0.5 μ m.

are frequently located in close proximity to M and P synapses in macaque monkeys. Unlike the case in owl monkeys, however, no differences were seen in the proportion of such synapses between M and P axons in macaque monkeys. Methodology may account for the differences in our results in owl monkeys and the results by Freund et al. (1989) in macaque monkeys. Freund et al. (1989) examined all contacts made by four completely reconstructed axons (2 P and 2 M axons), whereas we compared approximately 150 labeled LGN terminals with clear synapses of each type chosen from different blocks of tissue. Therefore, our sample may have been drawn from many different axons of each type, although the disadvantage of our data is that we sampled from single, not serial sections. Each sampling method has advantages and disadvantages, and both sampling methods could be biased based on relatively small numbers. It is also possible that the differences reflect true species differences, because significant size differences were found between M and P boutons in macaque monkeys; size differences that we do not find in the owl monkey.

In our material, M, P, and K axons not only differed with respect to their relationship to GABAergic profiles, but also showed other quantitative differences. As mentioned above, M and P axons are significantly larger than K axons and because terminal size appears to correlate with the number of synapses made by LGN terminals, M

and P axons can also be distinguished from K axons based on percentages of multiple synapses made.

Functional implications

The three parallel LGN pathways in owl monkey visual cortex (M, P, and K) terminate on separate sets of cortical neurons but appear to use similar basic operations at the first synapse. All three LGN axon classes communicate by means of glutamate and synapse preferentially with dendrites (typically spines) that also use glutamate. Such an arrangement is not surprising given that virtually all visual information used by the cortex must pass through these synapses. However, it has been argued that in layer IV of the macaque monkey, the spiny stellate cells (the main recipient cells of input from the LGN) receive only a small fraction of their input from the LGN (Peters and Payne, 1993). Presumably, the same holds true for input from M and P axons in owl monkeys given that other studies that have examined the proportion of thalamocortical synapses with spiny stellate cells also find that they account for only a small proportion of the total number of synapses on these cells (see Peters et al., 1994, for review). The argument has been made that geniculocortical signals are amplified by means of either intracortical circuits or circuits involving feedback to the LGN (Vidyasagar et al., 1996; Murphy and Sillito, 1996). If these amplification circuits involve only the spiny stellate cells of layer IV, the

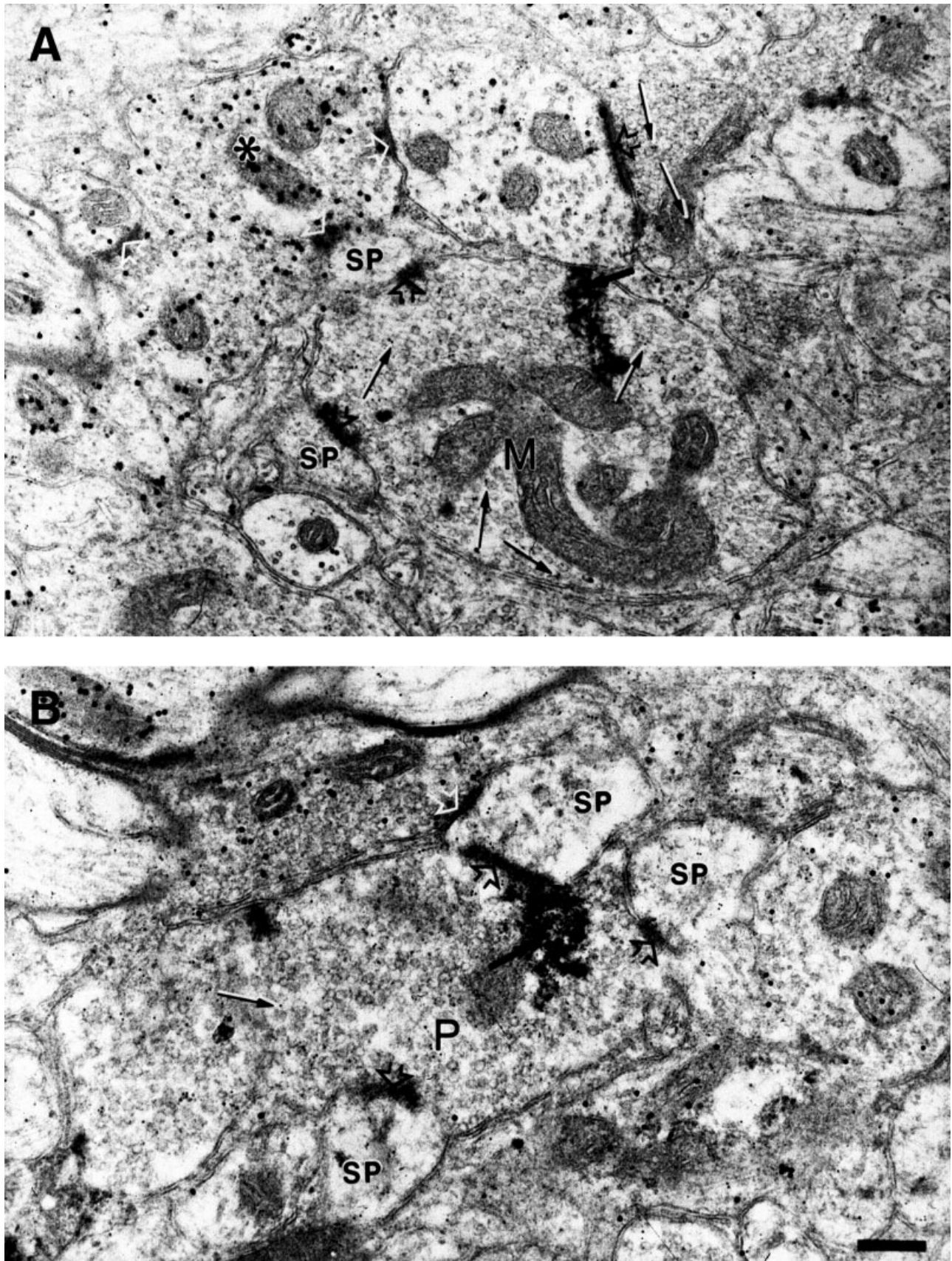


Fig. 10. M and P axons are often found in regions of layer IV α (A) and layer IV β (B), respectively, where they form a synaptic junction with other profiles that are engaged in complex synaptic relationships. Other conventions are as in Figure 1. Scale bar = 0.5 μ m in B (applies to A,B).

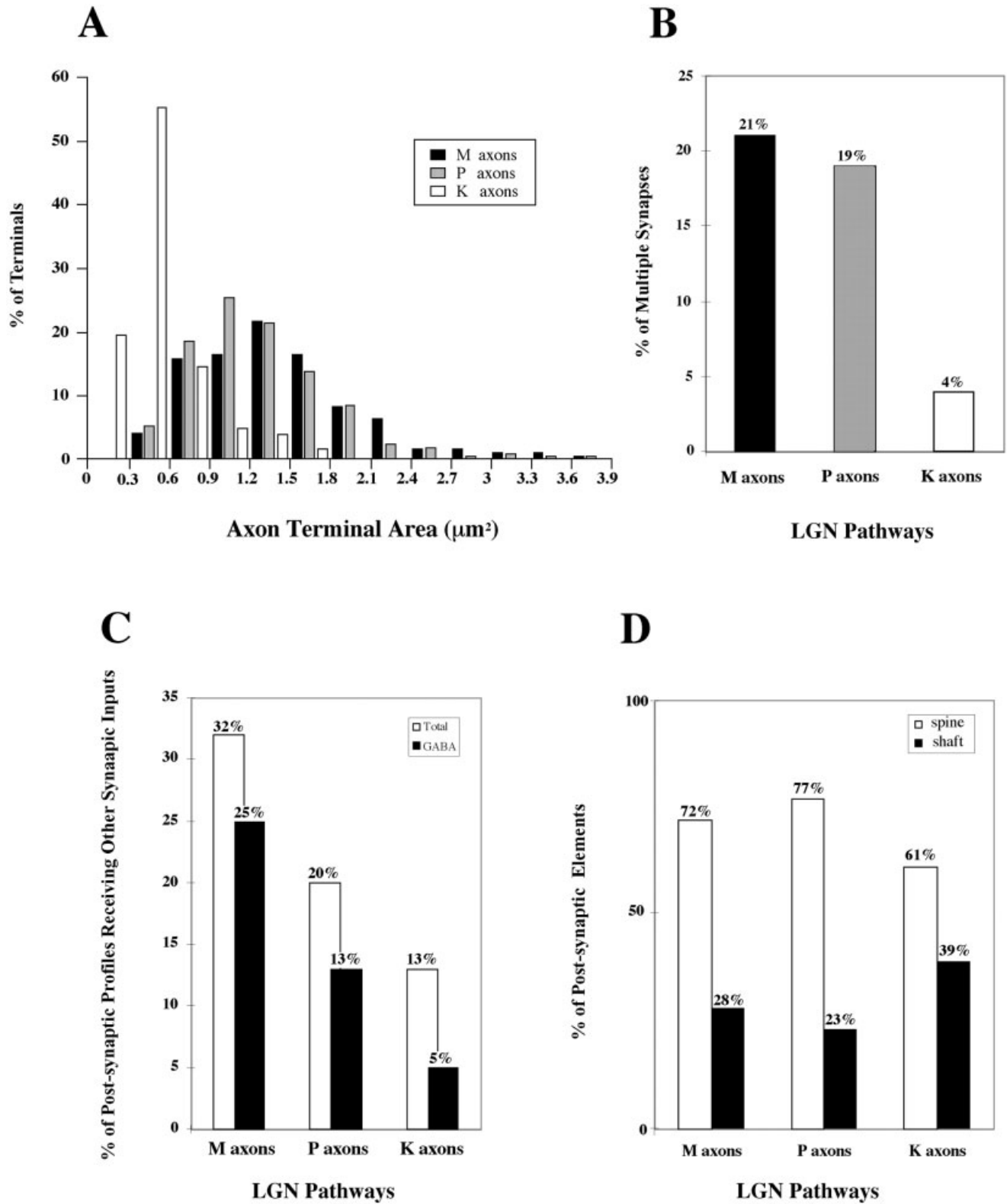


Fig. 11. Quantitative comparisons of magnocellular (M), parvocellular (P), and koniocellular (K) axons and their synaptic relationships. **A:** Histograms compare the size distributions of M, P, and K axon terminals. Only labeled terminals with at least one synaptic contact were measured. The average terminal areas of M axons ($\bar{x} = 1.40 \pm 0.65 \mu\text{m}^2$, $n = 176$) and P axons ($\bar{x} = 1.29 \pm 0.54 \mu\text{m}^2$, $n = 209$) are significantly larger (t test, $P \leq 0.00001$ for M and K; $P \leq 0.0001$ for P and K) than K axon terminal areas ($\bar{x} = 0.51 \pm 0.36 \mu\text{m}^2$, $n = 131$). **B:** Histograms compare the percentage of M, P, and K terminals that

exhibit multiple synapses. M and P axons exhibit multiple synapses much more frequently than do K axons. **C:** Histograms compare the percentage of dendrites postsynaptic with M, P, and K axons that receive additional synapses. In the single-section material, profiles postsynaptic to M axons receive more synapses than those postsynaptic to P axons, which, in turn, receive more synapses than those postsynaptic to K axons. **D:** Histograms compare the percentage of M, P, and K axons synapsing with dendritic spines and shafts. LGN, lateral geniculate nucleus; GABA, γ -aminobutyric acid.

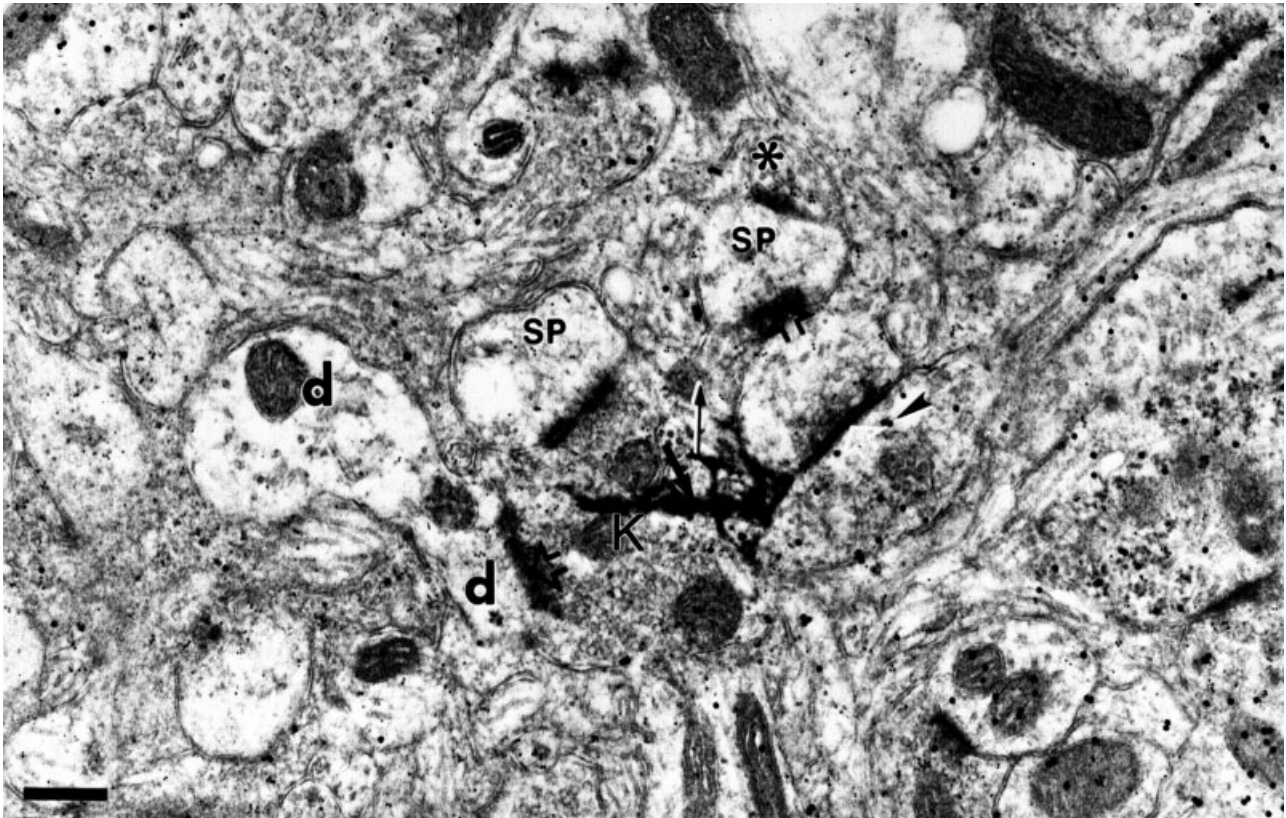


Fig. 12. Koniocellular (K) axons are often found in regions of the cytochrome oxidase blobs in layer III, where they form a synaptic junction with several other profiles (in this example, several spines and a small dendrite) that can be engaged in complex synaptic relationships. Other conventions are as in Figure 1. Scale bar = 0.5 μ m.

K pathway may operate differently from the M and P pathways because spiny stellate cells are absent in layer III (Lund, 1984). Thus, K axons, which terminate preferentially in the CO-blobs of layer III, must target the spines of either local layer III pyramidal cells or apical dendrites of pyramidal cells arising from cells in layer V (Ding and Casagrande, 1998). Regardless, it is clear that the ultimate impact of each of the LGN signals will depend upon knowing whether cells postsynaptic to M, P, and K LGN axons have similar or different types of glutamate receptors (Carder, 1997).

The receptive field properties of P, M, and K LGN cells in all primates studied, including owl monkeys, can be distinguished based on differences in spatial and temporal frequency selectivity, as well as other criteria (Sherman et al., 1976; Xu et al., 2001). Regardless of class, LGN cells can, in most cases, be distinguished from their cortical target cells. Most cells in V1 are orientation selective and are often also direction selective. How these new receptive field properties are constructed has been a matter of some debate (Bonds, 1989; Douglas and Martin, 1991; Ferster and Jagadeesh, 1991; Pei et al., 1994; Sompolinsky and Shapley, 1997). In macaque monkeys and squirrel monkeys, studies have shown that cells postsynaptic to LGN P axons within layer IV β have nonoriented receptive fields like their LGN inputs, whereas those located in layer IV α that receive input from M axons exhibit both orientation

and direction selectivity (Livingstone and Hubel, 1984; Blasdel and Fitzpatrick, 1984). These observations suggest either that M and P inputs are arranged differently or that other aspects of the circuitry in IV α and IV β differ (O'Keefe et al., 1998). There is evidence to suggest that inhibition plays a role in constructing orientation selectivity (Sillito, 1975; Allison and Bonds, 1994; Allison et al., 1995; Gibber et al., 2001; Roerig and Chen, 2002). Our present electron microscopic data in owl monkeys indicates that synaptic arrangements involving M, P, and K axons exhibit differences in relationship to cortical GABAergic circuitry. That M axons in owl monkeys are more likely to synapse with GABAergic dendrites or with dendrites receiving synaptic input from GABAergic interneurons than P axons are supports this view. In owl monkeys, K axons fall intermediate between M and P axons in these relationships to GABAergic circuits, as might be expected from the mixture of cell types and properties reported for the CO-blobs (Livingstone and Hubel, 1984; T'so and Gilbert, 1988; Lennie et al., 1990; DeBruyn et al., 1993; Leventhal et al., 1995).

V1 cells in layer IV postsynaptic to M and P axons clearly receive their main drive from the LGN; layer IV is traditionally considered to be the primary feedforward input layer in sensory cortex. On the other hand, the CO-blobs are primarily considered to be the source of cells within the output pathway to V2 in primates, not part of

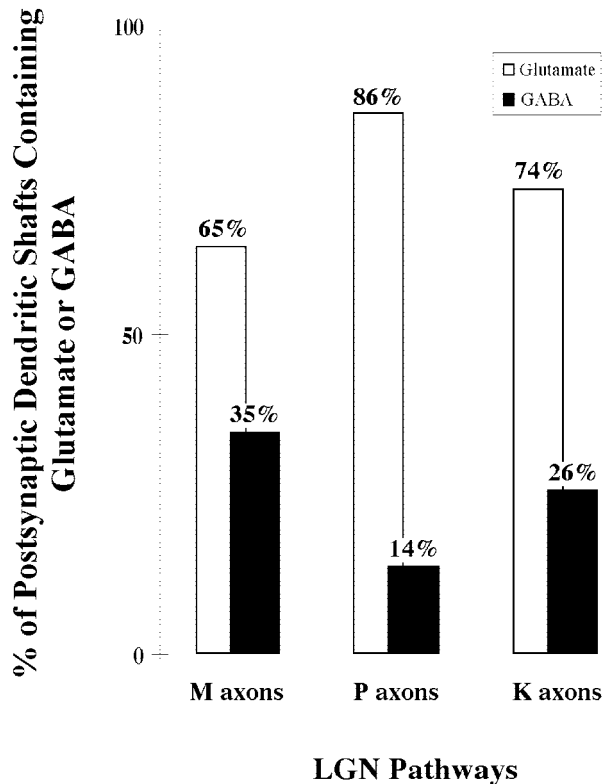


Fig. 13. Measures of interactions with inhibitory interneurons. Histogram shows the percentage of dendrites postsynaptic to labeled M, P, or K axons that contain glutamate or GABA. LGN, lateral geniculate nucleus; GABA, γ -aminobutyric acid; M, magnocellular, P, parvocellular; K, koniocellular.

the primary input circuit (Krubitzer and Kaas, 1990; Casagrande and Kaas, 1994). It remains unclear whether CO-blob cells postsynaptic to K axons are driven directly by the K pathway. CO-blobs in owl monkeys receive not only direct K input but also, as demonstrated by both our light and electron microscopic data, indirect input from M and P cellular targets in layer IV (Ding and Casagrande, 1998; Shostak et al., 2002). Thus, information from all three pathways is combined within these compartments. Of interest, the patterns of synaptic arrangements made by axons projecting from layer IV to the CO-blobs, which presumably carry the indirect signals from the M and P pathways, are distinct from those made by K LGN axons in these same compartments in several respects. Axons from layer IV are more likely to synapse with dendritic shafts than with spines, are smaller in size, and synapse with smaller dendritic shafts than do K axons (Shostak et al., 2002). These characteristics would suggest that axons from layer IV (indirect M & P input) are less likely to provide the main visual drive to CO-blob cells than K axons. However, qualitative estimates of the number of synapses provided by either axons from layer IV or axons from the K pathway suggest that the numbers of each are low and that the properties of CO-blob cells must reflect enormous influence from other cortical sources (Ding and Casagrande, 1998).

ACKNOWLEDGMENTS

We thank Julia Mavity-Hudson for her excellent technical and photographic assistance and Dr. Jamie Boyd for assistance in surgery. We also thank Drs. Ray Guillery, Tamas Freund, James McKanna, Jamie Boyd, Amy Wiencken-Barger, Jennifer Ichida, and Kelly Lusk for helpful comments on this article, and to Dr. Jan Rosemergy for proofing the article.

LITERATURE CITED

- Allison JD, Bonds AB. 1994. Inactivation of the infragranular striate cortex broadens orientation tuning of supragranular visual neurons in the cat. *Exp Brain Res* 101:415–416.
- Allison JD, Casagrande VA, Bonds AB. 1995. The influence of input from the lower cortical layers on the orientation tuning of upper layer V1 cells in a primate. *Vis Neurosci* 12:309–320.
- Blasdel GG, Fitzpatrick D. 1984. Physiological organization of layer 4 in macaque striate cortex. *J Neurosci* 4:880–895.
- Bonds AB. 1989. Role of inhibition in the specification of orientation selectivity of cells in the cat striate cortex. *Vis Neurosci* 2:41–55.
- Brodman K. 1909. *Vergleichende Lokalisationlehre der Grosshirnrinde in ihren Prinzipien dargestellt auf Grund des Zellenbaues*. Leipzig: JA Barth.
- Carder RK. 1997. Immunocytochemical characterization of AMPA-selective glutamate receptor subunits: laminar and compartmental distribution in macaque striate cortex. *J Neurosci* 17:3352–3363.
- Casagrande VA. 1994. A third parallel visual pathway to primate area V1. *Trends Neurosci* 17:305–310.
- Casagrande VA, Kaas JH. 1994. The afferent, intrinsic, and efferent connections of primary visual cortex in primates. In: Peters A, Rockland KS, editors. *Cerebral cortex*. New York: Plenum Press. p 201–259.
- Casagrande VA, Norton TT. 1991. Lateral geniculate nucleus: a review of its physiology and function. In: Leventhal AG, editor. *The neural basis of visual function*. London: Macmillan Press. p 41–84.
- Cruz-Orive LM. 1989. On the precision of systematic sampling: a review of Matheron's transitive methods. *J Microsc* 153:315–333.
- Cruz-Orive LM, Weibel ER. 1981. Sampling designs for stereology. *J Microsc* 122:235–257.
- DeBruyn EJ, Casagrande VA, Beck PD, Bonds AB. 1993. Visual resolution and sensitivity of single cells in the primary visual cortex (V1) of a nocturnal primate (bush baby): correlation with cortical layers and cytochrome oxidase patterns. *J Neurophysiol* 69:3–18.
- Diamond IT, Conley M, Itoh K, Fitzpatrick D. 1985. Laminar organization of geniculocortical projections in *Galago senegalensis* and *Aotus trivirgatus*. *J Comp Neurol* 242:584–610.
- Ding Y, Casagrande VA. 1997. The distribution and morphology of LGN K pathway axons within the layers and CO blobs of owl monkey V1. *Vis Neurosci* 14:691–704.
- Ding Y, Casagrande VA. 1998. Synaptic and neurochemical characterization of parallel pathways to the cytochrome oxidase blobs of primate visual cortex. *J Comp Neurol* 391:419–443.
- Douglas RJ, Martin KA. 1991. A functional microcircuit for cat visual cortex. *J Physiol* 440:735–769.
- Ferster D. 1988. Spatially opponent excitation and inhibition in simple cells of the cat visual cortex. *J Neurosci* 8:1172–1180.
- Ferster D, Jagadeesh B. 1991. Nonlinearity of spatial summation in simple cells of areas 17 and 18 of cat visual cortex. *J Neurophysiol* 66:1667–1679.
- Freund TF, Martin KAC, Whitteridge D. 1985a. Innervation of cat visual areas 17 and 18 by physiologically identified X- and Y-type thalamic afferents. I. Arborization patterns and quantitative distribution of postsynaptic elements. *J Comp Neurol* 242:263–274.
- Freund TF, Martin KAC, Somogyi P, Whitteridge D. 1985b. Innervation of cat visual areas 17 and 18 by physiologically identified X- and Y-type thalamic afferents. II. Identification of post-synaptic targets by GABA immunocytochemistry and Golgi Impregnation. *J Comp Neurol* 242: 275–291.
- Freund TF, Martin KAC, Soltesz I, Somogyi P, Whitteridge D. 1989. Arborization pattern and post-synaptic targets of physiologically identified thalamocortical afferents in striate cortex of the macaque monkey. *J Comp Neurol* 289:315–336.

- Garey LJ, Powell TPS. 1971. An experimental study of the termination of the lateral geniculo-cortical pathway in the cat and monkey. *Proc R Soc Lond Series B* 179:41–63.
- Gibber M, Chen B, Roerig B. 2001. Direction selectivity of excitatory and inhibitory neurons in ferret visual cortex. *Neuroreport* 12:2293–2296.
- Greenamyre JT, Porter RH. 1994. Anatomy and physiology of glutamate in the CNS. *Neurology* 44:S7–S13.
- Guillery RW. 1969. The organization of synaptic interconnections in the laminae of the dorsal lateral geniculate nucleus of the cat. *Z Zellforsch* 96:1–38.
- Guillery RW. 1971. Patterns of synaptic interconnections in the dorsal lateral geniculate nucleus of cat and monkey: a brief review. *Vision Res Suppl* 3:211–227.
- Hamos JE, Van Horn SC, Raczkowski D, Sherman SM. 1987. Synaptic circuits involving an individual retinogeniculate axon in the cat. *J Comp Neurol* 259:165–192.
- Hata Y, Tsumoto T, Sato H, Hagihara K, Tamura H. 1988. Inhibition contributes to orientation selectivity in visual cortex of cat. *Nature* 335:815–817.
- Horn AKE, Hoffmann K-P. 1987. Combined GABA-immunocytochemistry and TMB-HRP histochemistry of pretectal nuclei projecting to the inferior olive in rats, cats and monkeys. *Brain Res* 409:133–138.
- Hubel DH, Wiesel TN. 1962. Receptive fields, binocular interaction and functional architecture in the cat's visual cortex. *J Physiol* 160:106–154.
- Kaas JH, Lin C-S, Casagrande V. 1976. The relay of ipsilateral and contralateral retinal input from the lateral geniculate nucleus to striate cortex in the owl monkey: a transneuronal transport study. *Brain Res* 106:371–378.
- Katz LC. 1987. Local circuitry of identified projection neurons in cat visual cortex brain slices. *J Neurosci* 7:1223–1249.
- Kharazia VN, Weinberg RJ. 1994. Glutamate in thalamic fibers terminating in layer IV of primary sensory cortex. *J Neurosci* 14:6021–6032.
- Krubitzer L, Kaas J. 1990. Convergence of processing channels in the extrastriate cortex of monkeys. *Vis Neurosci* 5:609–613.
- Lachica EA, Casagrande VA. 1992. Direct W-like geniculate projections to the cytochrome oxidase (CO) blobs in primate visual cortex: axon morphology. *J Comp Neurol* 319:141–158.
- Lennie P, Krauskopf J, Sclar G. 1990. Chromatic mechanisms in striate cortex of macaque. *J Neurosci* 10:649–669.
- LeVay S, Gilbert CD. 1976. Laminar patterns of geniculocortical projection in the cat. *Brain Res* 113:1–19.
- Leventhal AG, Thompson KG, Liu D, Zhou Y, Ault SJ. 1995. Concomitant sensitivity to orientation, direction, and color of cells in layers 2, 3, and 4 of monkey striate cortex. *J Neurosci* 3:1808–1818.
- Livingstone MS, Hubel DH. 1984. Anatomy and physiology of a color system in the primate visual cortex. *J Neurosci* 4:309–356.
- Lund JS. 1984. Spiny stellate cells. In: Peter A, Jones EG, editors. *Cerebral cortex*. Vol. 1. Cellular components of the cerebral cortex. New York: Plenum. p 255–308.
- Merigan WH, Maunsell JHR. 1993. How parallel are the primate visual pathways? *Annu Rev Neurosci* 16:369–402.
- Mesulam M-M. 1978. Tetramethyl benzidine for horseradish peroxidase neurohistochemistry: a non-carcinogenic blue reaction-product with superior sensitivity for visualizing neural afferents and efferents. *J Histochem Cytochem* 26:106–117.
- Montero VM. 1990. Quantitative immunogold analysis reveals high glutamate levels in synaptic terminals of retino-geniculate, cortico-geniculate, and geniculo-cortical axons in the cat. *Vis Neurosci* 4:437–443.
- Montero VM. 1994. Quantitative immunogold evidence for enrichment of glutamate but not aspartate in synaptic terminals of retino-geniculate, geniculo-cortical, and cortico-geniculate axons in the cat. *Vis Neurosci* 11:675–681.
- Murphy PC, Sillito AM. 1996. Functional morphology of the feedback pathway from area 17 of the cat visual cortex to the lateral geniculate nucleus. *J Neurosci* 16:1880–1892.
- Nieuwenhuys R. 1994. The neocortex. An overview of its evolutionary development, structural organization and synaptology. *Anat Embryol (Berl)* 190:307–337.
- O'Keefe LP, Levitt JB, Kiper DC, Shapley RM, Movshon JA. 1998. Functional organization of owl monkey lateral geniculate nucleus and visual cortex. *J Neurophysiol* 80:594–609.
- Pei X, Vidyasagar TR, Volgushev M, Creutzfeldt OD. 1994. Receptive field analysis and orientation selectivity of postsynaptic potentials of simple cells in cat visual cortex. *J Neurosci* 14:7130–7140.
- Peters A, Feldman ML. 1977. The projection of the lateral geniculate nucleus to area 17 of the rat cerebral cortex. IV terminations upon spiny dendrites. *J Neurocytol* 6:669–689.
- Peters A, Payne BR. 1993. Numerical relationships between geniculocortical afferents and pyramidal cell modules in cat primary visual cortex. *Cereb Cortex* 3:69–78.
- Peters A, Payne BR, Budd J. 1994. A numerical analysis of the geniculocortical input to striate cortex in the monkey. *Cereb Cortex* 4:215–229.
- Phend KD, Weinberg RJ, Rustioni A. 1992. Techniques to optimize post-embedding single and double staining for amino acid neurotransmitters. *J Histochem Cytochem* 40:1011–1020.
- Pierce JP, Mendell LM. 1993. Quantitative ultrastructure of Ia boutons in the ventral horn: scaling and positional relationships. *J Neurosci* 13:4748–4763.
- Pospichal MW, Florence SL, Kaas JH. 1994. The postnatal development of geniculocortical axon arbors in owl monkeys. *Vis Neurosci* 11:71–90.
- Roerig B, Chen B. 2002. Relationships of local inhibitory and excitatory circuits to orientation preference maps in ferret visual cortex. *Cereb Cortex* 12:187–198.
- Sherman SM, Wilson JR, Kaas JH, Webb SV. 1976. X- and Y-cells in the dorsal lateral geniculate nucleus of the owl monkey (*Aotus trivirgatus*). *Science* 192:475–477.
- Shostak Y, Ding Y, Mavity-Hudson J, Casagrande VA. 2002. Cortical synaptic arrangements of the third visual pathway in three primate species: *Macaca mulatta*, *Saimiri sciureus*, and *Aotus trivirgatus*. *J Neurosci* 22:2885–2893.
- Sompolinsky H, Shapley R. 1997. New perspectives on the mechanisms for orientation selectivity. *Curr Opin Neurobiol* 7:514–522.
- Sillito AM. 1975. The contribution of inhibitory mechanisms to the receptive field properties of neurones in the striate cortex of the cat. *J Physiol* 250:305–329.
- Tigges M, Tigges J. 1979. Types of degenerating geniculocortical axon terminals and their contribution to layer IV in the squirrel monkey (*Saimiri*). *Cell Tissue Res* 196:4711–4786.
- T'so DY, Gilbert CD. 1988. The organization of chromatic and spatial interactions in the primate striate cortex. *J Neurosci* 8:1712–1727.
- Vidyasagar TR, Pei X, Volgushev M. 1996. Multiple mechanisms underlying the orientation selectivity of visual cortical neurones. *Trends Neurosci* 19:272–277.
- Winfield DA, Powell TPS. 1976. The termination of thalamo-cortical fibres in the visual cortex of the cat. *J Neurocytol* 5:269–281.
- Winfield DA, Powell TPS. 1983. Laminar cell counts and geniculo-cortical boutons in area 17 of cat and monkey. *Brain Res* 277:223–229.
- Winfield DA, Rivera-Dominguez M, Powell TPS. 1982. The termination of geniculocortical fibres in area 17 of the visual cortex in the macaque monkey. *Brain Res* 231:19–32.
- Wiser AK, Callaway EM. 1996. Contributions of individual layer 6 pyramidal neurons to local circuitry in macaque primary visual cortex. *J Neurosci* 16:2724–2739.
- Xu X, Ichida JM, Allison JD, Boyd JD, Bonds AB, Casagrande VA. 2001. A comparison of Koniocellular (K), Magnocellular (M), and Parvocellular (P) receptive field properties in the Lateral Geniculate Nucleus (LGN) of the Owl Monkey (*Aotus trivirgatus*). *J Physiol (Lond)* 531:203–218.